PCCP

Matrix isolation, time-resolved IR, and computational study of the photochemistry of benzoyl azide†‡

Elena A. Pritchina,[a] Nina P. Gritsan,*[a] Alexander Maltsev,[b] Thomas Bally,*[b] Tom Autrey,[c] Yonglin Liu,[d] Yuhong Wang[d] and John P. Toscano*[d]

[a] *Institute of Chemical Kinetics and Combustion, Siberian Branch of Russian Academy of Sciences and Novosibirsk State University, 630090 Novosibirsk, Russia*
[b] *Department of Chemistry, University of Fribourg, Pérolles, CH-1700 Fribourg, Switzerland*
[c] *Pacific Northwest National Laboratory, Richland, WA 99352, USA*
[d] *Department of Chemistry, Johns Hopkins University, Baltimore, MD 21218, USA*

Received 11th October 2002, Accepted 22nd November 2002
First published as an Advance Article on the web 16th December 2002

It was shown recently on the basis of DFT calculations (N. P. Gritsan and E. A. Pritchina, *Mendeleev Commun.*, 2001, **11**, 94) that the singlet states of aroylnitrenes undergo tremendous stabilization due to an extra N–O bonding interaction. To test experimentally the multiplicity and the structure of the lowest state of benzoylnitrenes we performed a study of their photochemistry in Ar matrices at 12 K. Formation of two species was observed on irradiation of benzoyl azide (**1b**) and its 4-acetyl derivative (**1c**). One of these species has an IR spectrum, which is consistent with that of isocyanate (**2b,c**). The IR and UV spectra of the second intermediate are in very good agreement with the calculated spectra of the singlet species (**3b,c**), whose structure is intermediate between that of a carbonylnitrene and an oxazirene. We further examined the photochemistry of benzoyl azide in solution at ambient temperatures by nanosecond time-resolved IR methods and obtained additional evidence for the singlet ground state of benzoylnitrene as well as insight into its reactivity in acetonitrile, cyclohexane, and dichloromethane. The above experiments were accompanied by quantum chemical calculations which included also a thorough investigation of the parent species, formylnitrene, at different levels of theory.

Introduction

It is well known that alkyl- and arylnitrenes have triplet ground states.[1] This is evident from the characteristic triplet EPR spectra of alkyl and arylnitrenes which have been observed in glassy matrices at 77 K.[1–3] However, the value of the singlet–triplet energy splitting (ΔE_{ST}) has been determined experimentally in only three cases. It was found to be 36 kcal mol^{-1} in the simplest nitrene, imidogen (NH),[4] 31 kcal mol^{-1} in methylnitrene[5] and about 18 kcal mol^{-1} in phenylnitrene.[6] Calculations have demonstrated that in contrast to phenylcarbene the lowest singlet state of phenylnitrene has an open-shell electronic configuration ($^1A_2$).[7,8]

The case of carbonylnitrenes is more complicated and inconsistent. Early studies[9–12] of the photochemistry of benzoyl azide in the presence of singlet nitrene traps (olefins, sulfides *etc.*) demonstrated formation of products typical of singlet nitrene reactions, along with a high yield of phenyl isocyanate, the product of a photo-Curtius rearrangement. However, product distributions in the presence of trapping agents and photosensitizers were interpreted to indicate a triplet ground state for benzoylnitrene.[10] On the other hand, Inagaki and co-workers[13] demonstrated that direct and triplet sensitized photolysis of benzoyl azide in *cis*- and *trans*-alkenes produces the same products characteristic for a singlet nitrene. Finally, no triplet EPR spectrum could be detected after photolysis of benzoyl azide in glassy matrices.[2,14]

In view of this inconsistency Schuster and co-workers undertook a comprehensive study of the photochemistry of naphthoyl- and substituted benzoyl azides in order to determine the multiplicity of the aroylnitrene ground state.[15–18] Although, they were unable to determine the multiplicity unambiguously, they concluded that their data leave little doubt that aroylnitrenes have a singlet ground state.[15,16] Based on this prediction they proposed acetyl- and nitro-substituted aroyl azides as potential photolabeling reagents.[17,18]

Recently we have performed DFT calculations on the properties of the singlet and triplet states of benzoyl and naphthoylnitrenes in order to understand the reasons for the tremendous stabilization of the singlet state in aroylnitrenes compared to arylnitrenes.[19] Thereby we found that the structure of the CON fragment in the lowest singlet state of benzoyl and naphthoylnitrenes ($^1A'$) shows the features of a cyclic oxazirene, although the N–O distance (~1.76 Å) is much longer than in a normal N–O single bond (about 1.4 Å or ~1.5 Å in strained cycles[20]). The energy difference between the singlet and triplet states of benzoylnitrene was found to be small, although the triplet state was still lower in energy by 5.4 kcal mol^{-1}.[19] Assuming that standard DFT calculations would overestimate ΔE_{ST}, we predicted that aroylnitrenes should indeed have singlet ground states. The reason for the dramatic stabilization of the $^1A'$ relative to the $^3A''$ state of aroylnitrenes

† Dedicated to Professor Dr Z. R. Grabowski and Professor Dr J. Wirz on the occasions of their 75th and 60th birthdays.

‡ Electronic supplementary information (ESI) available: Cartesian coordinates and details of the CASSCF/CASPT2 calculations, details of the excited-state calculations on formylnitrene, the full IR spectra, additional results from the TRIR experiments and two tables with results from CASPT2 calculations with different level shifts. See http://www.rsc.org/suppdata/cp/b2/b209775c/

 DOI: 10.1039/b209775c

appeared to be a special bonding interaction between the nitrogen and oxygen atoms which results in the structure of the singlet being intermediate between those of a nitrene and an oxazirene.

In this paper we report results of high level quantum chemical calculations of the properties of the lowest singlet and triplet states of formylnitrene which we undertook to understand the influence of the basis set and level of the theory on the calculated value of the singlet–triplet energy splitting (ΔE_{ST}) and to analyze the accuracy of simple DFT calculations. Thereby we found that B3LYP/6-31G* provides very good geometries for the singlet and triplet species in spite of the fact that it predictes $\Delta E_{ST} > 8$ kcal mol^{-1} for formylnitrene, in stark disagreement with our benchmark CCSD(T)/cc-pVQZ//CCSD(T)/cc-pVTZ calculations which give $\Delta E_{ST} = -0.13$ kcal mol^{-1}.

The main purpose of the present work is, however, to assess the multiplicity and the structure of the lowest state of benzoylnitrene and its 4-acetyl derivative by experimental means Thus we performed a study of the photochemistry of benzoyl azide in an Ar matrix at 12 K using UV–vis and IR spectroscopic detection of the products. Formation of two species was observed upon irradiation of benzoyl azide (**1b**) and its 4-acetyl derivative (**1c**). One of these species has an IR spectrum, which is consistent with that of the isocyanates, **2**, whereas, the IR and UV spectra of the second intermediate are in very good agreement with the calculated spectra of the singlet species **3**.

We also examined the photochemistry of benzoyl azide in solution at ambient temperatures by nanosecond time-resolved infrared (TRIR) spectroscopy. In agreement with calculations and low-temperature matrix IR experiments, we have observed an IR band consistent with singlet **3b** and have examined the reactivity of **3b** in acetonitrile, cyclohexane, and dichloromethane.

Experimental

Benzoyl azide was synthesized from benzoyl chloride following the published procedure[21] and purified by recrystallization from acetone. 4-Acetylbenzoyl azide was prepared from 4-acetylbenzoic acid by the procedure of ref. 16.

Spectroscopy in argon matrices

A gaseous mixture of 1 part of benzoyl azide in 1000 parts of argon (mixed with 10% of nitrogen to improve the optical properties of the matrix) was slowly deposited on a CsI plate at 19 K. In the case of 4-acetylbenzoyl azide a few ground crystals of azide were placed in a U-tube just before the inlet system of the cryostat. During deposition the temperature of U-tube was about 20 °C. The gas mixture flowed through the U-tube to carry along appropriate quantities of 4-acetylbenzoyl azide to form a matrix giving reasonable optical densities of azide and products of its photolysis.

Photolysis of benzoyl azide and 4-acetylbenzoyl azide was performed with a low-pressure mercury (254 nm) or a medium-pressure Hg/Xe lamp with a 313-nm or 365 nm interference filters.

Electronic absorption spectra were obtained on a Perkin-Elmer Lambda-900 spectrometer (200–1000 nm). IR spectra were measured on a Bomem DA3 interferometer (4000–500 cm^{-1}) with an MCT detector.

Time-resolved IR spectroscopy

TRIR experiments were conducted (with 16 cm^{-1} spectral resolution) following the method of Hamaguchi and co-workers,[22] as has been described previously.[23] The error in reported rate constants is ±10%.

Quantum chemical calculations

The B3LYP/6-31G* geometries of singlet and triplet formylnitrene and benzoylnitrene were taken from our previous computational study[19] and those of the other compounds discussed in this study (4-acetylbenzoyl azide, 4-acetyl-, 4-amino- and 4-nitrobenzoylnitrenes, phenyl- and 4-acetylphenylisocyanate) were computed at the same level (the resulting Cartesian coordinates are listed in the electronic supplementary information (ESI)‡). All structures were ascertained to be minima on the potential energy surfaces by second derivative calculations which also yielded harmonic frequencies (for comparison with experimental spectra) and zero-point energies which were taken into account in the calculations of singlet–triplet splittings. The stability of the SCF solutions for the nitrenes was tested by CIS calculations.[24]

The singlet–triplet energy splitting of formylnitrene was also evaluated at the CCSD and CCSD(T) levels of theory[25] with Dunning's correlation-consistent basis sets ranging from double to quadruple-zeta quality.[26] All of these calculations were performed with the Gaussian-98 suite of programs,[27] except for the geometry optimization of formylnitrene at the CCSD(T) level which was carried out with the ACES II program.[28]

Excited state energies were calculated at the same geometries by the CASSCF/CASPT2 procedure[29] with the ANO-S basis set of Pierloot *et al.*[30a] The active space used in these calculations is shown in Figs. 4 and 5, below. In order to arrive at a satisfactory description of all excited states at the CASPT2 level (*i.e.* to remove intruder states) it was necessary to resort to the level-shifting technique,[30b] whereby it was carefully assured that no artifacts are introduced (Tables T3–T4 of the ESI‡ describe the results of calculations carried out with level shifts ranging from 0 to 0.3 au). All CASSCF/CASPT2 calculations were carried out with the MOLCAS 4 suite of programs.[31]

To predict the electronic absorption spectra of singlet and triplet 4-acetylbenzoylnitrene we resorted to the time-dependent (TD) DFT method[32] (as implemented in the Gaussian program[32c]) with the B3LYP combination of exchange and correlation functionals[33] using the 6-31+G* basis set.

Results and discussion

Quantum chemical calculations on formylnitrene

As was shown in our previous paper[19] the geometry of the C(O)N fragment in the lowest singlet and triplet states of nitrenes R–C(O)N and the singlet–triplet splittings (ΔE_{ST}) were relatively insensitive to the replacement of the hydrogen atom by a phenyl or a naphthyl group. Therefore, the results of high-level calculations for formylnitrene (HCON) may be generalized to the case of aroylnitrenes.

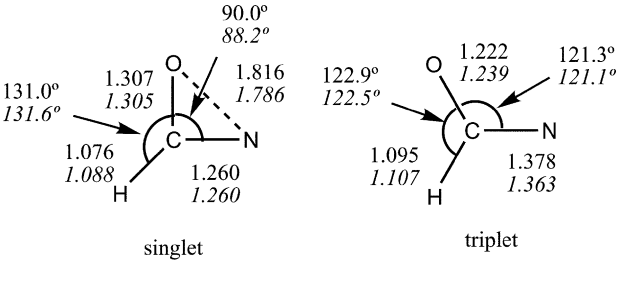

Fig. 1 Bond lengths (Å) and bond angles in the singlet A′ (left) and the triplet A″ states (right) of formylnitrene, calculated by CCSD(T)/cc-pVTZ (normal font) and by B3LYP/6-31G* (italic).

Table 1 The singlet–triplet splitting (ΔE_{ST}) calculated without ZPE correction[a] using different methods, basis sets and formylnitrene geometries

Method	ΔE_{ST}/kcal mol^{-1}
B3LYP/6-31G*	8.14
B3LYP/cc-pVDZ[b]	8.53
B3LYP/cc-pVTZ[b]	6.79
B3LYP/cc-pVQZ[b]	6.65
B3LYP: complete basis set extrapolation[c]	6.64
CCSD/cc-pVDZ[d]	14.09
CCSD/cc-pVTZ[d]	11.01
CCSD/cc-pVQZ[d]	9.93
CCSD: complete basis set extrapolation[c]	9.35
CCSD(T)/6–31G*[d]	3.47
CCSD(T)/cc-pVDZ[d]	5.21
CCSD(T)/cc-pVTZ[d]	1.15
CCSD(T)/cc-pVQZ[d]	−0.13
CCSD(T): complete basis set extrapolation[c]	−0.72

[a] The zero point energy of singlet formylnitrene is higher than that of triplet formylnitrene by 0.8 kcal mol^{-1} according to B3LYP and by 0.5 kcal mol^{-1} by CCSD(T), both with the 6-31G* basis set. [b] At the B3LYP/6-31G* geometry; [c] Complete basis set extrapolation was performed using the Dunning–Feller formula;[34] [d] At the CCSD(T)/cc-pVTZ geometry.

The geometry of HCON in the lowest singlet and triplet states was now reoptimized at the CCSD(T)/cc-pVTZ level of theory. Fig. 1 shows that the resulting geometries agree very well with those found by the above DFT procedure, *i.e.* B3LYP/6-31G* provides adequate geometries of the lowest singlet and triplet states of carbonylnitrenes.

The singlet–triplet splittings ($\Delta E_{ST} = E_S - E_T$) for formylnitrene calculated at different levels of theory are presented in Table 1. B3LYP and CCSD calculations provide strongly positive ΔE_{ST} (*i.e.* they predict triplet ground states), whereby the gap is slightly reduced on going to larger basis sets. On the other hand, ΔE_{ST} decreases dramatically on perturbative inclusion of triple excitations in the coupled cluster scheme, and the further reduction on increasing the basis set leads to an extrapolated value (for a complete basis set[34]) of $\Delta E_{ST} = -0.72$ kcal mol^{-1}. However, on adding the difference in zero point energies ΔE_{ST} goes back to nearly zero, so we must conclude that even very high-level calculations do not allow us to make any firm prediction with regard to the ground state multiplicity of formylnitrene. What we *can* conclude is that the two spin states must lie very close in energy, and that B3LYP overestimates ΔE_{ST} in formylnitrene by about 9 kcal mol^{-1} if the 6-31G* basis set is used. In any event the expected proximity of the two spin states will make for very interesting experimental results.

The ΔE_{ST} value for benzoylnitrene calculated by B3LYP/6-31G* is positive (5.4 kcal mol^{-1}),[19] but about 3 kcal mol^{-1} smaller than that for formylnitrene. Similar values were calculated for a series of *para*-substituted benzoylnitrenes (Table 2). However, the previous experimental date of Schuster *et al.* on the photochemistry of acetyl- and nitro-substituted benzoyl azides,[16–18] as well as our own experimental results described below indicate a *singlet* ground state for benzoyl nitrenes.

Table 2 The singlet–triplet splitting (ΔE_{ST}) with ZPE corrections for benzoylnitrene and its 4-substituted (RC_6H_4CON) derivatives calculated using B3LYP/6-31G* method

RC_6H_4CON	R=H	R=C(O)CH$_3$	R=NH$_2$	R=NO$_2$
ΔE_{ST}/kcal mol^{-1}	5.44	5.64	5.68	6.10

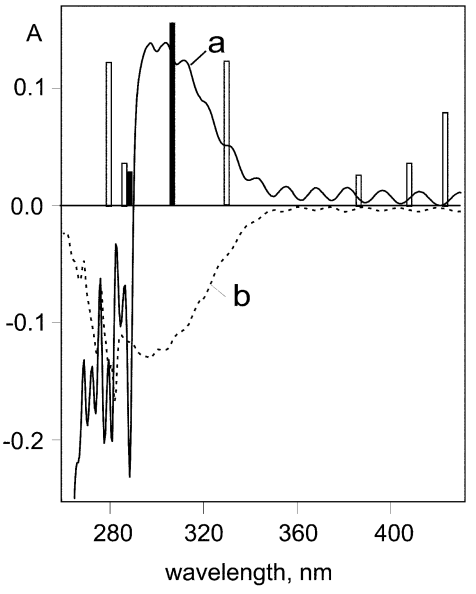

Fig. 2 Changes in the optical spectrum on 254 nm photolysis of benzoyl azide (**1b**) in an Ar matrix at 12 K for 2 min (a) and changes in spectrum a upon 8 min irradiation at 313 nm (b). Computed positions and relative oscillator strengths (see Table 3) of the absorption bands of the singlet species **3b** are depicted as solid bars, those of triplet benzoyl nitrene as open bars.

Therefore the overestimation of ΔE_{ST} by B3LYP must be of a similar magnitude in benzoylnitrene as it is in formylnitrene.

The failure to detect a triplet EPR spectrum upon photolysis of benzoyl azide in glassy matrices[2,14] was only indirect evidence of singlet nitrene formation. Only direct spectroscopic identification of the singlet species can solve this problem. Thus, we performed a study of the photochemistry of benzoyl azide both in an Ar matrix at 12 K using UV–vis and IR spectroscopic detection of products, and in solution at room temperature using nanosecond TRIR spectroscopy.

Photolysis of benzoyl azide, 1: Spectroscopy in argon matrices

After 2 minutes of photolysis in Ar at 254 nm, the optical spectrum of benzoyl azide **1b** was replaced by a new band with a maximum around 300 nm (Fig. 2, spectrum a). Simultaneously, the IR bands of **1b**, in particular the strong 2145 cm^{-1} N_3 stretching vibration, disappeared almost completely and gave way to a set of new peaks, notably a strong group around 2270 cm^{-1} (Fig. 3).

Subsequent irradiation at 313 nm led to the disappearance of the newly formed UV-band (Fig. 2, spectrum b). Concomitantly some of the newly formed IR peaks diminished strongly (Fig. 3, spectra b, negative peaks), whereas some other peaks, notably the intense group around 2270 cm^{-1}, continued to grow. Thus this experiment indicates very clearly the formation of at least two products on 254 nm photolysis. The first of these products has an absorption maximum at ~300 nm and rearranges to the other primary product on exposure to 313 nm light.

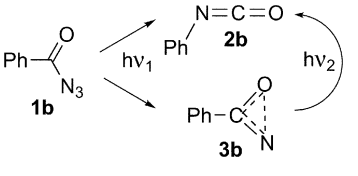

Scheme 1

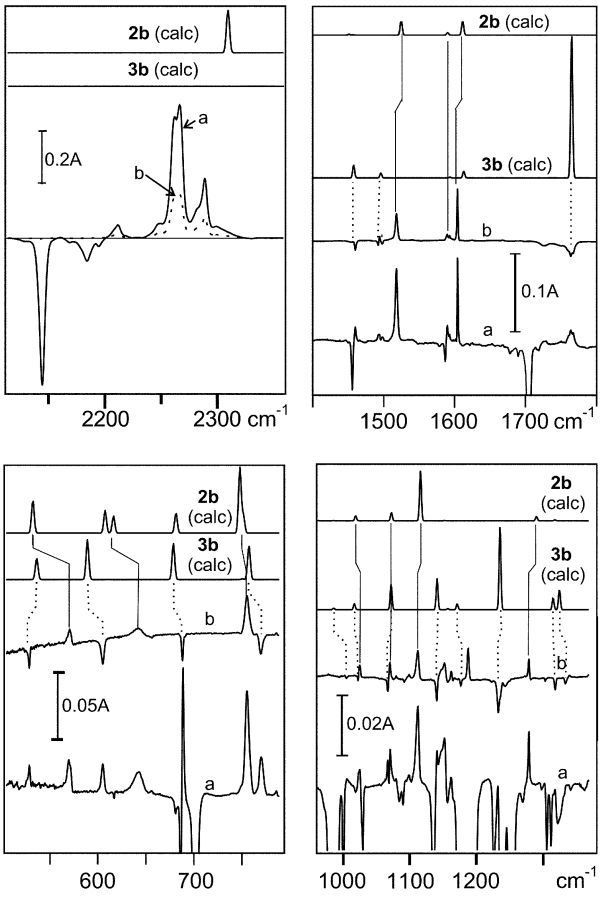

Fig. 3 Changes in four diagnostic IR-regions upon 254 nm photolysis of benzoyl azide (**1b**) in an Ar matrix at 12 K for 2 min (a) and subsequent 313 nm photolysis for 8 min (b). The top two traces of each panel show the IR spectra of singlet **3b** and phenylisocyanate **2b** calculated by the B3LYP/6-31G* and scaled by 0.97.

The formation of phenylisocyanate (**2b**), along with products derived from singlet benzoylnitrene, is well known to occur upon photolysis of benzoyl azide at room temperature.[9–13] Therefore we assume that the products of the photolysis of **1b** at 12 K are isocyanate **2b** and the singlet species **3b** which is in turn converted to isocyanate on subsequent photolysis.

Next to the very intense doublet at 2266/2289 cm^{-1} the IR spectrum of the final product has many less intense peaks[35] in the range of 500–1800 cm^{-1} (Fig. 3). All of them correlate well with the spectrum calculated for phenylisocyanate **2b** (solid lines). The only exception, a small peak at 1193 cm^{-1}, coincides with one of the most intense peaks of the azide precursor and is therefore probably an artifact due to the spectral subtraction. Note that B3LYP predicts a single intense peak at 2310 cm^{-1} for **2b** (Fig. 3), although the spectrum of **2b** in CCl_4 also contains a very intense doublet[36] at 2260 and 2278 cm^{-1}. Thus the doublet observed in the Ar matrix is not due to site splitting, but probably due to a Fermi resonance.

The optical spectrum of **2b** has two maxima at 269 and 277 nm,[14b] in agreement with the absence of appreciable absorptions of the final products above 280 nm (Fig. 2). Thus the absorption band at about 300 nm belongs presumably to the singlet species **3b**. Indeed, the two most intense transitions in the spectrum of **3b** calculated by the CASSCF/CASPT2 procedure are at 306 and 290 nm, respectively (solid bars in Fig. 2, Table 3). In addition a very weak transition to the first excited state is predicted at 513 nm. It consists mainly of electron promotion from an allylic type π-orbital to the low lying σ*-orbital of the very weak NO-bond.

The IR spectrum of the species[37] with the absorption maximum at 300 nm (Fig. 3, Spectrum b, negative peaks) is also in very good agreement with the calculated IR spectrum of **3b** (Fig. 3, dotted lines). In contrast, the calculated IR spectrum of triplet benzoylnitrene shows no relation to this experimental IR spectrum (*cf.* Fig. S2 in the ESI‡). For instance, it has no absorptions in the vicinity of 1765 cm^{-1}, whereas its most intense bands are predicted at 1206 and 1513 cm^{-1}, a region where no intense experimental peaks were recorded.

We have also calculated the UV–vis spectrum of triplet benzoylnitrene, using the CASSCF/CASPT2 procedure (Table 4). Triplet phenyl nitrene exhibits a strong absorption band in the near UV region with a maximum at 308 nm.[38] Two transitions contribute to this absorption and the main configurations contributing to one of them involves excitation of an electron from the sp-lone pair orbital to the singly occupied in-plane 2p orbital of the nitrogen atom. This transition is very similar to those observed from the triplet ground states of parent NH (336 nm),[39] methylnitrene (315 nm),[40] perfluoromethylnitrene (354 nm)[41] and 1-norbornylnitrene (298 nm).[42] In view of this we added three a′ orbitals (the singly occupied in-plane p-orbital of nitrogen, and two combinations of the in-plane oxygen and nitrogen lone pairs) to the eight orbitals of a″-type (π and π*) in the active space (Fig. 5).

It is seen from Table 4 that triplet benzoylnitrene is predicted to have several intense absorption bands in the visible and near-UV region. This spectrum shows no relation to the experimental one (*cf.* open bars in Fig. 2) and we take this to confirm the absence of the triplet benzoylnitrene among the products of photolysis of **1b**.

Therefore, two products, phenylisocyanate (**2b**) and a singlet species **3b** with a structure intermediate between that of a nitrene and an oxazirene, are produced on photolysis of

Table 3 Vertical excitation energies of singlet benzoylnitrene **3b** calculated by the CASSCF(12,11)[a]/CASPT2 method[b] at the B3LYP/6-31G* geometries

State	E_{CASSCF}/eV	E_{CASPT2}[b]/eV	Ref. weight[c]	λ/nm	f[d]	Major configurations[e]
$1^1A'$	0.0	0.0	0.77			75% of ground configuration
$1^1A''$	2.76	2.42	0.76	513	1.2×10^{-4}	78%: 4a″ → 27a′
$3^1A'$	4.86	4.06	0.75	306	3.0×10^{-2}	41%: 3a″ → 6a″
$2^1A'$	4.71	4.27	0.75	290	4.9×10^{-3}	30%: 5a″ → 6a″
						15%: 4a″ → 7a″
$2^1A''$	5.52	4.97	0.75	250	8.2×10^{-7}	30%: 5a″ → 27a′ + 4a″ → 7a″
						21%: 3a″ → 27a′ + 4a″ → 6a″
$3^1A''$	6.01	5.09	0.75	244	2.2×10^{-5}	34%: 3a″ → 27a′
						15%: 4a″ → 27a′ + 4a″ → 6a″

[a] Active space includes 9 a″ and 2 a′ orbitals, the most important of which are shown in Fig. 4; [b] Calculated with a level shift of 0.25 au, see Table T3 in the ESI for more details; [c] weight of the zero-order CASSCF wavefunction in the CASPT2 expansion;. [d] Oscillator strength for electronic transition, based on the CASSCF wave functions and the CASPT2 energy differences. [e] In a (12,11) CASSCF wavefunction; orbitals see Fig. 4.

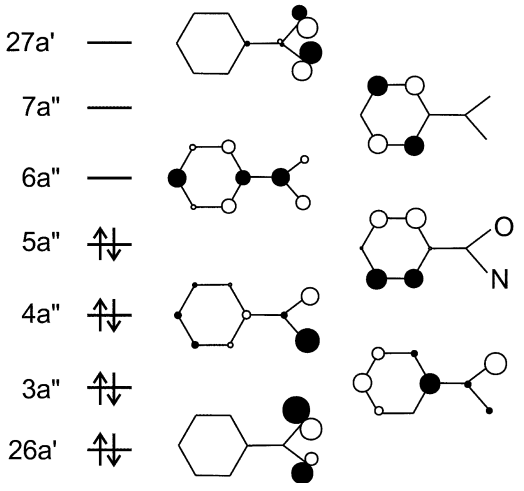

Fig. 4 Orbitals involved in the electronic transitions of singlet species **3b** (*cf.* Table 3).

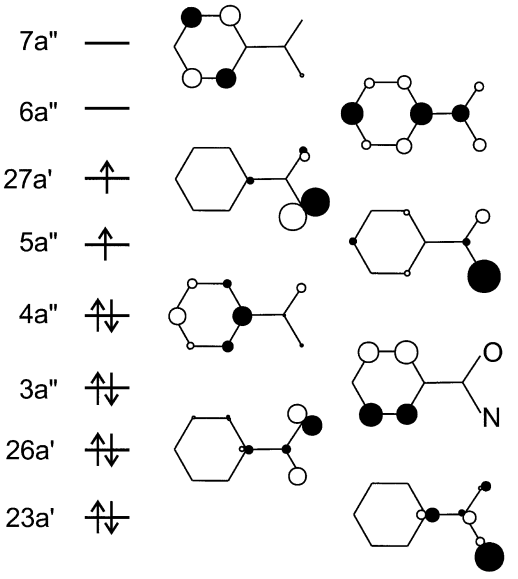

Fig. 5 Orbitals involved in the electronic transitions of triplet benzoylnitrene (*cf.* Table 4).

benzoyl azide. According to the IR spectral data about 75% of isocyanate **2b** is formed after complete decomposition of benzoyl azide (2 min of 254 nm photolysis), and full conversion to **2b** is achieved after 313 nm bleaching of **3b**. Using the initial slope of the kinetics for the formation of **2b** and **3b** on 254 nm irradiation we can estimate the ratio of **2b/3b** in the primary process as being 64 to 36%.

Note that, similar to the case of triplet benzoylnitrene, triplet formylnitrene has also intense absorption bands in visible and near UV region, whereas the singlet species, **3a**, only absorbs appreciably in the UV region, with a maximum at about 260 nm. The detailed analysis of the calculated UV–vis spectra of **3a** and triplet formylnitrene is presented in the ESI (Tables S1 and S2 and Figs. S1 and S2).‡

Photolysis of benzoyl azide, 2: Time-resolved IR studies

Typical TRIR data observed following 266 nm laser excitation of azide **1b** in argon-saturated acetonitrile-d_3 are shown in Fig. 6 for the spectral region 1800–1200 cm^{-1}. Kinetic traces for the positive bands centered at 1760, 1635, 1570, and 1515 cm^{-1} are shown in Fig. 7. (Kinetic traces observed at 1320 cm^{-1} are identical to those observed at 1635 cm^{-1}.)

The negative bands detected at 1696 and 1248 cm^{-1} are due to depletion of **1b**. On the basis of the calculations and matrix studies discussed above, we assign the positive band at 1760 cm^{-1} to singlet nitrene **3b**. Additional evidence that the 1760 cm^{-1} band is due to a singlet species is that its rate of decay is completely unaffected by oxygen (see ESI‡). In acetonitrile, **3b** decays ($k_{decay} = 3.0 \times 10^6$ s^{-1}) to an intermediate species with very strong IR bands at 1635 and 1320 cm^{-1} ($k_{growth} = 3.4 \times 10^6$ s^{-1}). The decay rate of these bands ($k_{decay} = 4.1 \times 10^4$ s^{-1}) matches the growth rate for a band observed at 1570 cm^{-1} ($k_{growth} = 4.4 \times 10^4$ s^{-1}). (Note that the fast growth component observed at this frequency is due to overlap with the tail of the strong 1635 cm^{-1} band; see Fig. 6.) Abraham and co-workers have demonstrated that the product of reaction of **3b** and acetonitrile is 2-methyl-5-phenyl-1,3,4-oxadiazole.[43] Thus, we assign the 1570 cm^{-1}

Table 4 Vertical excitation energies of triplet benzoylnitrene calculated using the CASSCF(12,11)[a]/CASPT2 method at the B3LYP/6-31G* geometry

State	E_{CASSCF}/eV	E_{CASPT2}[b]/eV	Ref. weight[c]	λ/nm	f[d]	Major configurations[e]
$1\ ^3A''$	0.0	0.0	0.75			83% of ground configuration
$1\ ^3A'$	0.45	1.60	0.76	775	1.3×10^{-4}	80%: $26a' \rightarrow 5a''$
$2\ ^3A''$	3.21	2.93	0.74	424	1.4×10^{-2}	34%: $4a'' \rightarrow 5a''$
						21%: $4a'' \rightarrow 6a''$
$3\ ^3A''$	3.76	3.04	0.74	407	5.6×10^{-3}	72%: $23a' \rightarrow 27a'$
$4\ ^3A''$	3.81	3.21	0.74	386	4.6×10^{-3}	44%: $3a'' \rightarrow 5a''$
						10%: $3a'' \rightarrow 6a''$
$5\ ^3A''$	4.34	3.75	0.74	330	2.6×10^{-2}	36%: $3a'' \rightarrow 7a''$
						20%: $4a'' \rightarrow 5a''$
$6\ ^3A''$	4.61	4.32	0.74	287	6.4×10^{-3}	37%: $3a'' \rightarrow 6a''$
						19%: $4a'' \rightarrow 7a''$
$7\ ^3A''$	4.98	4.42	0.74	280	2.2×10^{-2}	21%: $5a'' \rightarrow 6a + 4a'' \rightarrow 5a''$
						17%: $4a'' \rightarrow 6a''$
$2\ ^3A'$	3.38	4.48	0.76	277	1.4×10^{-4}	35%: $27a' \rightarrow 6a''$
						17%: $26a' \rightarrow 27a' + 26a' \rightarrow 6a''$
$3\ ^3A'$	4.03	5.15	0.76	241	1.2×10^{-5}	27%: $5a'' \rightarrow 6a'' + 26a' \rightarrow 5a''$
						16%: $26a' \rightarrow 6a''$

[a] Active space includes 8 a″ and 3 a′ orbitals, the most important of which are shown in Fig. 5; [b] Calculated with a level shift of 0.25 au, see Table T4 in the ESI for more details; [c] weight of the zero-order CASSCF wavefunction in the CASPT2 expansion;. [d] Oscillator strength for electronic transition, based on the CASSCF wave functions and the CASPT2 energy differences. [e] In a (12,11) CASSCF wavefunction; orbitals in Fig. 5.

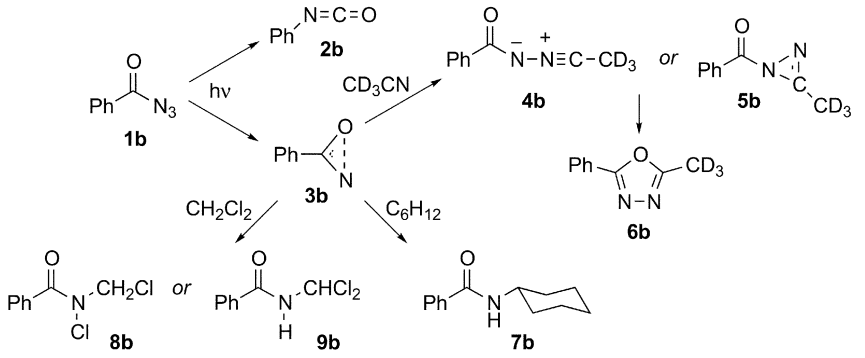

Scheme 2

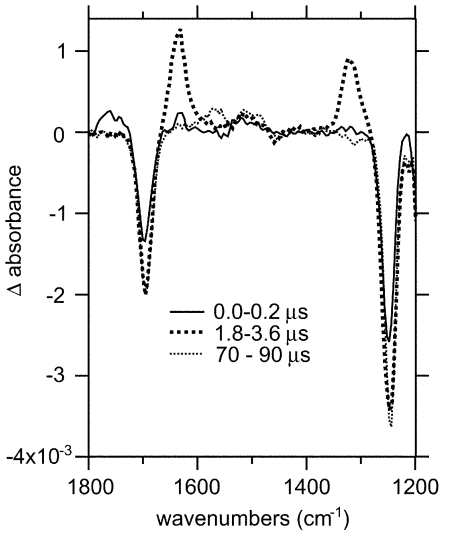

Fig. 6 TRIR difference spectra averaged over the timescales indicated following 266 nm laser photolysis (5 ns, 2 mJ) of azide **1b** (3.3 mM) in argon-saturated acetonitrile-d_3. Additional spectral data are given as ESI.‡

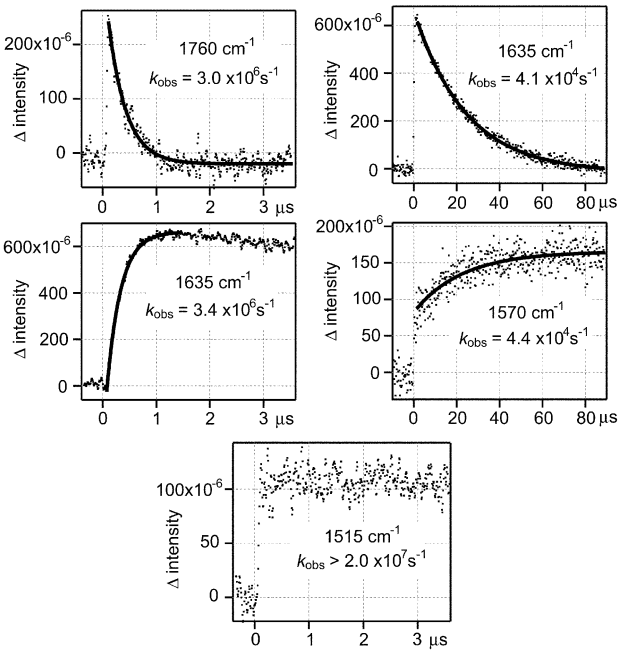

Fig. 7 Kinetic traces observed at 1760, 1635, 1570, and 1515 cm^{-1} following 266 nm laser photolysis (5 ns, 2 mJ) of azide **1b** (3.3 mM) in argon-saturated acetonitrile-d_3. The dotted curves are experimental data; the solid curves are the calculated best fit to a single exponential function.

band to oxadiazole **6b**, in good agreement with the reported[44] literature frequency of 1580 cm^{-1}.

Nitrile ylides and 1-acylazirines have been proposed as possible intermediates in the reaction of acylnitrenes with acetonitrile.[43,45] To help determine the identity of the intermediate observed in our acetonitrile TRIR experiments, we performed B3LYP/6-31G* calculations on ylide **4b** and azirine **5b**. Intense calculated IR bands (scaled by 0.96)[46] are predicted at 1661 and 1259 cm^{-1} for ylide **4b**, and at 1689 and 1225 cm^{-1} for azirine **5b**. On this basis, we tentatively assign our experimentally observed bands at 1635 and 1320 cm^{-1} to ylide **4b**.

As has been discussed previously, the initial species formed upon photolysis of azide **1b** are nitrene **3b** and isocyanate **2b**. To support the previous experimental work of Lwowski and co-workers, who demonstrated that *t*-butyl isocyanate does not arise from pivaloylnitrene, but rather from pivaloyl azide,[47,48] we wished to obtain direct kinetic evidence that isocyanate **2b** arises from an excited state of azide **1b** (or an electronically or vibrationally excited nitrene), rather than from the relaxed ground state of nitrene **3b**. We have conducted analogous experiments concerning the role of non-carbene precursors to ketenes in Wolff rearrangement chemistry.[49] Due to strong solvent IR absorbance above 2200 cm^{-1} in acetonitrile, we are unable to monitor the kinetics of the diagnostic high frequency isocyanate band. However, we do detect a weak band at 1515 cm^{-1} (Figs. 6 and 7), consistent with the calculated and experimentally observed IR spectrum of isocyanate **2b**.[50] This band grows in at a rate beyond our current time resolution (50 ns), confirming that the precursor of the isocyanate is not nitrene **3b**. Analogous results are found in cyclohexane (Fig. 8) and dichloromethane (Fig. 9), where the 2265 cm^{-1} isocyanate band is now easily detected. (TRIR spectral data in cyclohexane and dichloromethane are provided in the ESI.‡)

We also detected singlet nitrene **3b** in cyclohexane and dichloromethane. In cyclohexane **3b** ($k_{decay} = 1.1 \times 10^6$ s^{-1}) undergoes a C–H insertion reaction with solvent to give amide **7b** with strong absorption at 1680 cm^{-1} ($k_{growth} = 1.0 \times 10^6$ s^{-1}).[51] In dichloromethane **3b** ($k_{decay} = 1.6 \times 10^5$ s^{-1}) presumably undergoes a C–Cl or C–H insertion reaction with solvent to give amide **8b** or **9b**, respectively with absorption at 1718 cm^{-1} ($k_{growth} = 2.0 \times 10^5$ s^{-1}). (Preliminary experiments in Freon-113 (1,1,2-trichlorotrifluoroethane) reveal an analogous IR band at 1730 cm^{-1}.) B3LYP/6-31G* calculations predict (after scaling by 0.96)[46] an intense IR band at 1689 cm^{-1} for **8b**[52] and at 1708 cm^{-1} for **9b**. (We do not favor assignment of the 1718 cm^{-1} band to a nitrene **3b**-dichloromethane chloro-ylide since calculations predict an intense IR band at 1627 cm^{-1} for this species.) Abraham and co-workers have found that aroyl azides give 100% isocyanate upon photolysis in dichloromethane,[43] but that the addition of electron-rich olefins[53] or C_{60}[54] results in the formation of nitrene adducts. They, therefore, propose[43] that amide **8b** is formed, but

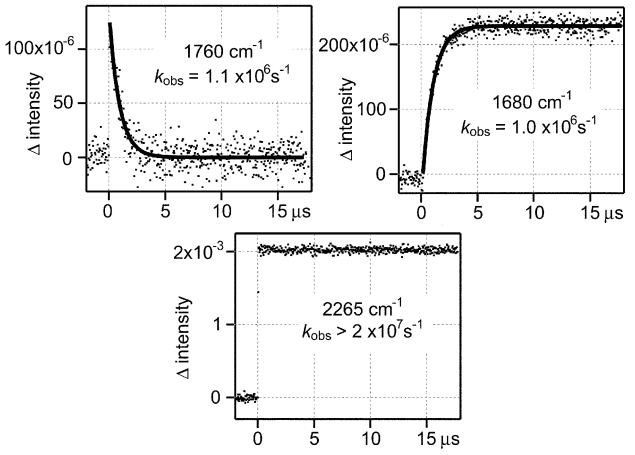

Fig. 8 Kinetic traces observed at 1760, 1680, and 2265 cm^{-1} following 266 nm laser photolysis (5 ns, 2 mJ) of azide **1b** (3.3 mM) in argon-saturated cyclohexane. The dotted curves are experimental data; the solid curves are the calculated best fits to a single exponential function.

subsequently decays to isocyanate **2b**. We do not observe decay of the experimentally observed 1718 cm^{-1} IR band to the isocyanate on the timescale of our TRIR experiments; it is stable for at least 200 μs. In addition, the lifetime of nitrene **3b** does not seem to be strongly affected by the initial concentration of azide **1b**; thus, changing the concentration of azide **1b** by a factor of six leaves the lifetime of **3b** unchanged.

Photolysis of 4-acetylbenzoyl azide (1c) in argon matrices

The concomitant formation of isocyanates from the photo-Curtius rearrangement of aroyl azides restricts their potential use in practical applications. Fortunately, Schuster and co-workers[16] found that irradiation of 4-acetylbenzoyl azide (**1c**) and 4-acetyl-4′-biphenoyl azide into their $n \rightarrow \pi^*$ bands ($\lambda > 345$ nm) gives only products that originate from the resulting nitrenes, whereas irradiation of the same azides into their $\pi \rightarrow \pi^*$ bands (254 nm) leads also to photo-Curtius rearrangement to form isocyanates. The excited triplet state of **1c** was detected chemically and by transient spectroscopic techniques. It was proposed that nitrogen loss following near-UV irradiation ($\lambda > 345$ nm) occurs exclusively from the excited triplet state of **1c**. However, products are consistent only with reactions originating from the singlet nitrene.[16]

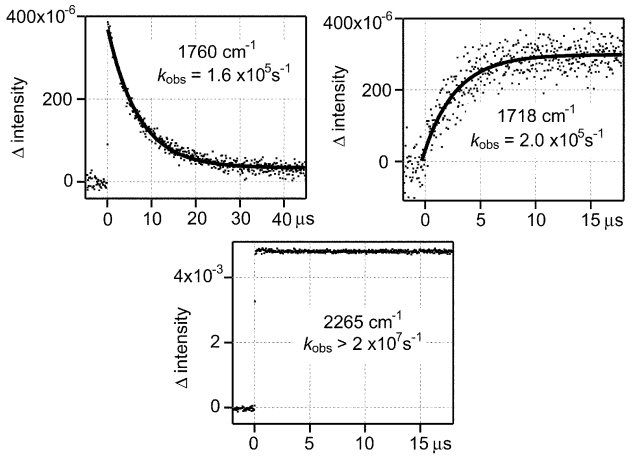

Fig. 9 Kinetic traces observed at 1760, 1718, and 2265 cm^{-1} following 266 nm laser photolysis (5 ns, 2 mJ) of azide **1b** (3.3 mM) in argon-saturated dichloromethane. The dotted curves are experimental data; the solid curves are the calculated best fits to a single exponential function.

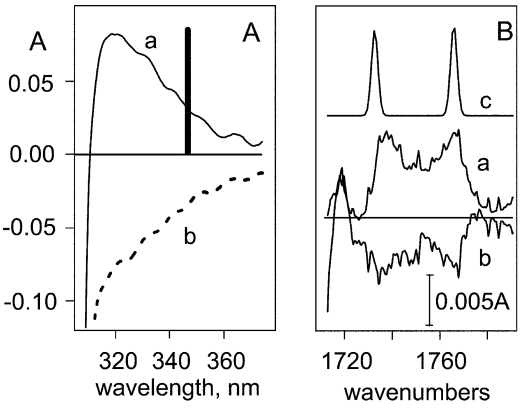

Fig. 10 (A) Changes in the optical spectrum obtained after the first 10 min (a) and after an additional 10 min (b) of 313 nm irradiation of 4-acetylbenzoyl azide **1c** in an argon matrix at 12 K. The position of the first absorption band of the singlet species **3c**, calculated by TD-B3LYP (see Table 5) is depicted as a solid line. (B) Differential IR spectra recorded under the same conditions as the optical spectra in panel A. The peaks shown in trace (c) are the two strongest IR transitions of the singlet species **3c** according to B3LYP/6-31G* calculations (energies scaled by 0.97).

Based on these findings we decided to study also the photochemistry of **1c** in Ar matrices. In order to avoid formation of isocyanate **2c** we excited **1c** into its $n \rightarrow \pi^*$ excited state at 365 nm. Unfortunately the $n \rightarrow \pi^*$ band of 4-acetylbenzoyl azide **1c** has a very low intensity (λ_{max} *ca.* 350, ε_{max} *ca.* 50 M^{-1} cm^{-1}).[16] Therefore, the singlet species, **3c**, formed upon photolysis of **1c** in Ar at 365 nm, absorbs this light and undergoes subsequent transformation. Only a very small absorption band with a maximum at ~320 nm was formed after 1 hour of 365 nm irradiation of **1c**, and this band disappeared on further irradiation. Note that two small peaks in the IR spectrum (1737, 1766 cm^{-1}) could be assigned with confidence to the intermediate with the 320 nm band in the UV spectrum. The IR spectrum of the final product (after 6 h of 365 nm photolysis) had a very intense peak at 2264 cm^{-1}, typical of isocyanate **2c**.

Unlike benzoyl azide, **1b**, which was decomposed almost completely after 2 min of 254 nm photolysis, its 4-acetyl derivative **1c** was only about 80% converted after 100 min of exposure to the same light. The low efficiency of photolysis of **1c** could be due to the triplet multiplicity of its reactive state.[16] It is known that N–N dissociation is very inefficient in the triplet states of aryl azides.[54,55] For instance, the quantum yields of the triplet-sensitized photolyses of phenyl azide[56] and *p*-dimethylaminophenyl azide[54] are significantly lower than those of the direct photolyses.

Similar to the case of 365 nm irradiation, an absorption band with a maximum at ~320 nm and two small peaks in IR spectrum (1737, 1766 cm^{-1}) appeared during the initial stages of 254 nm photolysys and were bleached on further irradiation. The IR spectrum of the final products, after 100 min

Table 5 Electronic absorption spectrum of singlet benzoylnitrene **3b** and its 4-acetyl derivative **3c** calculated by the time dependent (TD) B3LYP/6-31+G* method

	Benzoylnitrene		4-Acetylbenzoylnitrene	
Transitions	λ/nm	f	λ/nm	f
$S_0 \rightarrow S_1$	533	5.0×10^{-4}	534	5.0×10^{-4}
$S_0 \rightarrow S_2$	306	4.3×10^{-2}	362	0.0
$S_0 \rightarrow S_3$	280	0.0	342	6.0×10^{-2}
$S_0 \rightarrow S_4$	276	2.0×10^{-4}	287	1.0×10^{-4}

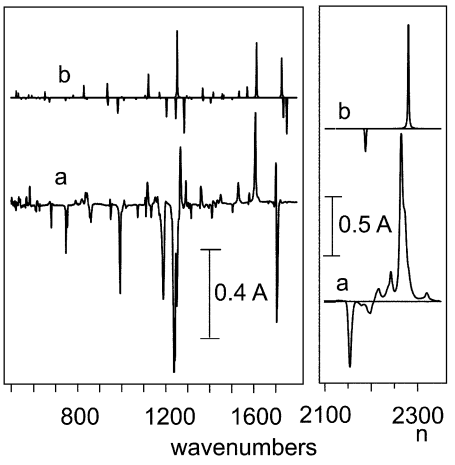

Fig. 11 The differential IR spectrum produced by exposure of 4-acetylbenzoyl azide (**1c**) in an Ar matrix at 12 K to 313 nm light for 20 min (a). Negative peaks are due to the disappearance of the azide. Positive peaks are due to the photoproduct. The IR spectra of azide (**1c**, negative peaks) and phenyl isocyanate (**2c**, positive peaks) are calculated (b) by the B3LYP/6-31G* method and scaled by 0.97.

of photolysis at 254 nm, consists of bands that were assigned to isocyanate **2c**, along with some unidentified peaks.

A larger yield of the intermediate could be accumulated by irradiation of **1c** at 313 nm, as illustrated below. Spectrum a of Fig. 10A corresponds to 10 min of photolysis. During the subsequent 10 min of irradiation, the 320 nm band disappeared almost completely (Fig. 10A, Spectrum b), along with two IR bands at 1737, 1766 cm^{-1} (Fig. 10B, Spectra a, b). According to our calculations the IR spectrum of the singlet species **3c** has its most intense peaks at 1732 and 1766 cm^{-1} (Fig. 10B, Spectrum c), *i.e.* very close to the experimental ones. According to the time dependent DFT calculations (Table 5) the UV absorption band of **3c** has a maximum at 342 nm, which agrees fairly well with the experimental one (Fig. 10A).

The final product of the photolysis of **1c** has an IR spectrum, which coincides very well with the calculated spectrum of 4-acetylphenylisocyanate **2c** (Fig. 11). Therefore, much like the case of benzoyl azide **1b**, two products, isocyanate **2c** and a singlet species **3c** with a structure intermediate between those of a nitrene and an oxazirene, are produced on photolysis of 4-acetylbenzoyl azide **1c**.

Acknowledgements

The authors are grateful to Russian Foundation for Basic Research (Grant 01-03-32864) and Swiss National Science Foundation (project No 2000-061560-00 and SCOPES grant No 7SUPJ062336). The group at Johns Hopkins thanks the US National Science Foundation (Grant CHE-0209350). T. A. thanks the US Office of Science, Office of Basic Energy Sciences, Chemical Sciences Division.

References

1 *Azides and Nitrenes. Reactivity and Utility*, ed. E. F. V. Scriven, Academic Press, New York, 1984.
2 E. Wasserman, G. Smolinsky and W. A. Yager, *J. Am. Chem. Soc.*, 1964, **86**, 3166.
3 E. Wasserman, *Prog. Phys. Org. Chem.*, 1971, **8**, 319.
4 P. C. Engelking and W. C. Lineberger, *J. Chem. Phys.*, 1976, **65**, 4323.
5 M. J. Travers, D. C. Cowles, E. P. Clifford, G. B. Ellison and P. C. Engelking, *J. Chem. Phys.*, 1999, **111**, 5349.
6 M. J. Travers, D. C. Cowles, E. P. Clifford and G. B. Ellison, *J. Am. Chem. Soc.*, 1992, **114**, 8699.
7 S.-J. Kim, T. P. Hamilton and H. F. Schaefer, *J. Am. Chem. Soc.*, 1992, **114**, 5349.
8 W. L. Karney and W. T. Borden, *J. Am. Chem. Soc.*, 1997, **119**, 1378.
9 R. Puttner and K. Hafner, *Tetrahedron Lett.*, 1964, 3119.
10 Y. Hayashi and D. Swern, *J. Am. Chem. Soc.*, 1973, **95**, 5205.
11 E. Eibler and J. Sauer, *Tetrahedron Lett.*, 1974, 2569.
12 V. P. Semenov, A. N. Studenikov, A. D. Bespalov and K. A. Ogloblin, *J. Org. Chem. USSR (Engl. Transl.)*, 1977, **12**, 2052.
13 (*a*) M. Inagaki, T. Shingaki and T. Nagai, *Chem. Lett.*, 1981, 1419; (*b*) M. Inagaki, T. Shingaki and T. Nagai, *Chem. Lett.*, 1982, 9.
14 (*a*) G. Smolinsky, E. Wasserman and W. A. Yager, *J. Am. Chem. Soc.*, 1962, **84**, 3220; (*b*) V. J. Kuck, E. Wasserman and W. A. Yager, *J. Phys. Chem.*, 1972, **76**, 3570.
15 T. Autrey and G. B. Schuster, *J. Am. Chem. Soc.*, 1987, **109**, 5814.
16 M. E. Sigman, T. Autrey and G. B. Schuster, *J. Am. Chem. Soc.*, 1988, **110**, 4297.
17 I. Woelfle, B. Sauerwein, T. Autrey and G. B. Schuster, *Photochem. Photobiol.*, 1988, **47**, 497.
18 T. Melvin and G. B. Schuster, *Photochem. Photobiol.*, 1990, **51**, 155.
19 N. P. Gritsan and E. A. Pritchina, *Mendeleev Commun.*, 2001, **11**, 94.
20 (*a*) A. I. Kitaigorodski, P. M. Zorki and V. K. Belski, *Structure of the Organic Compounds. Data of Structure Study. 1929–1970*, Science, Moscow, 1980, pp. 198, 199, 297, 298, 306–308; (*b*) A. I. Kitaigorodski, P. M. Zorki, and V. K. Belski, *Structure of the Organic Compounds. Data of Structure Study. 1971–1973*, Science, Moscow, 1982, p. 145.
21 E. W. Barrett and C. W. Porter, *J. Am. Chem. Soc.*, 1941, **63**, 3434.
22 (*a*) K. Iwata and H. Hamaguchi, *Appl. Spectrosc.*, 1990, **44**, 1431; (*b*) T. Yuzawa, C. Kato, M. W. George and H. Hamaguchi, *Appl. Spectrosc.*, 1994, **48**, 684.
23 (*a*) Y. Wang, T. Yuzawa, H. Hamaguchi and J. P. Toscano, *J. Am. Chem. Soc.*, 1999, **121**, 2875; (*b*) J. P. Toscano, *Adv. Photochem.*, 2001, **26**, 41.
24 If no precautions were taken, the triplet wavefunction invariably converged to an excited state. Reoptimization of the wavefunction with "stable = opt" led to the lowest triplet state.
25 (*a*) J. Cizek, *Adv. Chem. Phys.*, 1969, **14**, 35; (*b*) G. D. Purvis and R. J. Bartlett, *J. Chem. Phys.*, 1982, **76**, 1910; (*c*) G. E. Scuseria and H. F. Schaefer, III, *J. Chem. Phys.*, 1989, **90**, 3700.
26 D. E. Woon and T. H. Dunning, *J. Chem. Phys.*, 1993, **98**, 1358.
27 M. J. Frisch *et al.*, *Gaussian 98, Revisions A.6-A11*, Gaussian, Inc., Pittsburgh, PA, 1998.
28 J. F. Stanton, J. Gauss, J. D. watts, W. J. Lauderdale and R. J. Bartlett, *Int. J. Quant. Chem. Symp.*, 1992, **26**, 879.
29 K. Andersson and B. O. Roos, in *Modern Electronic Structure Theory*, World Scientific, Singapore, 1995, part 1, vol. 2, pp. 55.
30 (*a*) K. Pierloot, B. Dumez, P.-O. Widmark and B. O. Roos, *Theor. Chim. Acta*, 1995, **90**, 87; (*b*) B. O. Roos, K. Andersson, M. P. Fülscher, L. Serrano-Andrés, K. Perloot, M. Merchàn and V. Molina, *J. Mol. Struct (THEOCHEM)*, 1996, **388**, 257.
31 K. Andersson, M. R. A. Blomberg, M. P. Fülscher, V. Kellö, R. Lindth, P.-A. Malmqvist, J. Noga, B. O. Roos, A. Sadlej, P. L. M. Siegbahn, M. Urban and P.-O. Widmark, *MOLCAS, Version 3 and 4*, University of Lund, Sweden, 1994.
32 (*a*) E. K. U. Gross and W. Kohn, *Adv. Quant. Chem.*, 1990, **21**, 255; (*b*) M. E. Casida, in *Recent Advances in Density Functional Methods*, ed. D. P. Chong, World Scientific, Singapore, 1995, vol. 1; (*c*) K. B. Wiberg, R. E. Stratmann and M. J. Frisch, *Chem. Phys. Lett*, 1998, **297**, 60.
33 (*a*) A. D. Becke, *J. Chem. Phys.*, 1993, **98**, 5648; (*b*) C. Lee, W. Yang and R. G. Parr, *Phys. Rev. B.*, 1988, **37**, 785.
34 (*a*) T. H. Dunning, Jr., *J. Chem. Phys.*, 1989, **90**, 1007; (*b*) D. A. Feller, *J. Chem. Phys.*, 1992, **96**, 6104; (*c*) M. P. de Lara-Castells, R. V. Krems, A. A. Buchachenko, G. Delgado-Barrio and P. Villarreal, *J. Chem. Phys.*, 201, 115, 10438.
35 570, 642, 755, 904, 1028, 1074, 1117, 1285, 1517 and 1604 cm^{-1}.
36 H. Hoyer, *Chem. Ber.*, 1956, **89**, 2677.
37 529, 606, 689, 770, 1071, 1145, 1238, 1325, 1341, 1459 and 1765 cm^{-1}.
38 N. P. Gritsan, Z. Zhu, C. M. Hadad and M. S. Platz, *J. Am. Chem. Soc.*, 1999, **121**, 1202.
39 P. W. Fairchild, G. P. Smith, D. R. Crosly and J. B. Jeffries, *Chem. Phys. Lett.*, 1984, **107**, 181.
40 P. G. Carrick and P. C. Engelking, *J. Chem. Phys.*, 1984, **81**, 1661.
41 N. P. Gritsan, I. Likhotvorik, Z. Zhu and M. S. Platz, *J. Phys. Chem. A*, 2001, **105**, 3039.

42 J. G. Radziszewski, J. W. Downing, C. Wentrup, P. Kaszynski, M. Jawdosiuk, P. Kovacic and J. Michl, *J. Am. Chem. Soc.*, 1985, **107**, 2799.
43 K.-U. Clauss, K. Buck and W. Abraham, *Tetrahedron*, 1995, **51**, 7181.
44 (*a*) T. Chiba and M. Okimoto, *J. Org. Chem.*, 1992, **57**, 1375; (*b*) R. Y. Yang and L.-X. Dai, *J. Org. Chem.*, 1993, **58**, 3381.
45 W. Lwowski, A. Hartenstein, C. deVita and R. L. Smick, *Tetrahedron Lett.*, 1964, 2497.
46 A. P. Scott and L. Radom, *J. Phys. Chem.*, 1996, **100**, 16 502.
47 G. T. Tisue, S. Linke and W. Lwowski, *J. Am. Chem Soc.*, 1967, **89**, 6303.
48 S. Linke, G. T. Tisue and W. Lwowski, *J. Am. Chem. Soc.*, 1967, **89**, 6308.
49 Y. Wang and J. P. Toscano, *J. Am. Chem. Soc.*, 2000, **122**, 4512.
50 C. O. Kappe, G. Kollenz and C. Wentrup, *Acta Chem. Scand.*, 1993, **47**, 940.
51 The experimental IR frequency of amide **7b** (neat) is reported to be 1660 cm^{-1} B. M. Choudary, A. D. Prasad, V. Bhuma and V. Swapna, *J. Org. Chem.*, 1992, **57**, 5841.
52 The related *N*-chlorobenzamide is reported to have a strong IR band at 1699 cm^{-1} in dichloromethane W. J. deKlein, *Spectrochim. Acta, Part A*, 1972, **28**, 687.
53 K. Buck, D. Jacobi, Y. Plögert and W. Abraham, *J. Prakt. Chem.*, 1994, **336**, 678.
54 J. Averdung, J. Mattay, D. Jacobi and W. Abraham, *Tetrahedron*, 1995, **51**, 2543.
55 (*a*) A. K. Schrock and G. B. Schuster, *J. Am. Chem. Soc.*, 1984, **106**, 5228; (*b*) E. Leyva, M. S. Platz, G. Persy and J. Wirz, *J. Am. Chem. Soc.*, 1986, **108**, 3783.
56 (*a*) T. Kobayashi, N. Ohtani, K. Suzuki and T. Yamaoka, *J. Phys. Chem.*, 1985, **89**, 776; (*b*) C. J. Shields, D. E. Falvey, G. B. Schuster, O. Buchardt and P. E. Nielsen, *J. Org. Chem.*, 1988, **53**, 3501.